*Polish Journal of Chemical Technology, 19, **4**, 22—27, 10.1515/pjct-2017-0063*

Galvanic coupling effects for module-mounting elements of ground-mounted photovoltaic power station

Boguslaw Pierozynski[1], Henryk Bialy[2]

[1]*University of Warmia and Mazury in Olsztyn, Department of Chemistry, Faculty of Environmental Protection and Agriculture, Plac Lodzki 4, 10-727 Olsztyn, Poland*
[2]*Corab Limited, M. Kajki 4, 10-547 Olsztyn, Poland*
[*]*Corresponding author: e-mail: bogpierozynski@yahoo.ca; boguslaw.pierozynski@uwm.edu.pl*

This communication reports on the concerns associated with possible generation of galvanic coupling effects for construction materials that are used to manufacture mounting assemblies for ground-mounted photovoltaic (PV) power stations. For this purpose, six macro-corrosion galvanic cells were assembled, including: hot-dip Zn/Magnelis®-coated steel/Al and stainless steel (SS)/Al cells. Corrosion experiments involved continuous, ca. three-month exposure of these couplings in 3 wt.% NaCl solution, conducted at room temperature for a stable pH value of around 8. All corrosion cells were subjected to regular assessment of galvanic current-density and potential parameters, where special consideration was given to compare the corrosion behaviour of Zn-coated steel samples with that of Magnelis®-coated electrodes. Characterization of surface condition and elemental composition for examined materials was carried-out by means of SEM and EDX spectroscopy techniques.

Keywords: PV mounting assembly, Zn-coated steel, Magnelis® coating, galvanic coupling.

INTRODUCTION

Ground-mounted assemblies of photovoltaic (PV) power station modules generally consist of frames attached to mounting supports, which typically include concrete-embedded pole mounts. The PV solar modules are typically designed to last 25–30 years; thus, similar durability (mechanical and corrosion-related) is also expected from structural components of the photovoltaic system. Key elements of the PV racking arrangement include different metals and metal composites, namely: Zn-coated steel, Al sheets and profiles, stainless steel (SS) and copper fasteners[1–3]. A phenomenon of galvanic corrosion typically takes place when two dissimilar metals (or alloys) in a galvanic series are connected in the presence of electrolyte. An anode is more negative than a cathode in the galvanic series and thus it undergoes dissolution (anodic oxidation process), whereas oxygen (or H_3O^+) reduction proceeds at the cathode side. Generally, the further apart the metals are in the galvanic series, the greater the corrosion potential in the galvanic cell would be. However, the rates of electrochemical reaction between two metals are strictly dependent on electrolyte composition and its pH, and ambient temperature[4–7]. Hence, as the galvanic coupling between the two metals could significantly increase the corrosion rate of the anode, it is of superior importance that electrically shorted metal parts are not susceptible to galvanic corrosion.

In this work, we have examined the galvanic coupling behaviour for most representative couplings that could be found in PV-based installations. These included: hot-dip Zn(Magnelis®)-coated steel//Al and SS//Al galvanic couples, corrosion-tested at room temperature in 3 wt. % NaCl solution, a typical corrosion test electrolyte. Magnelis® is an innovative, composite Zn-based metallic coating, modified with 3.5% Al and 3% Mg. Magnelis® was originally introduced by ArcelorMittal company and as such it offered superior to typical Zn coatings protection in a number of corrosion environments[8].

EXPERIMENTAL

The work described in this communication involved characterization of the galvanic coupling effects for six galvanic cells, which imitate the PV structure/fastening connections, as described below:

1. Magnelis®-coated steel (S250GD: 1.0242 grade)// Al_{ox} (oxidized aluminum alloy);
2. Magnelis®-coated steel (S250GD: 1.0242 grade)// Al_{EF} (electrophoretically-coated aluminum alloy);
3. Hot-dip Zn-coated steel (DD11: 1.0332 grade)//Al_{ox};
4. Hot-dip Zn-coated steel (DD11: 1.0332 grade)//Al_{EF};
5. AISI 304 SS (304/0H18N9)//Al_{ox};
6. AISI 304 SS (304/0H18N9)//Al_{EF};

Samples of commercial Zn(Magnelis®)-coated steel sheets, aluminum and stainless steel specimens were prepared as follows:

– Hot-dip Zn-coated steel: 50×50×3.15 mm (*ca*. 80–90 μm Zn thickness);

– Magnelis®-coated steel: 50×50×3.02 mm (ArcelorMittal; *ca*. 25–30 μm thick coating);

– Al_{ox} (anodized Al 6063-T6 alloy): 50×50×3.85 mm, where Al anodization procedure was carried-out potentiostatically (0.5–1.0 V/SCE for constant charge of 1 C versus Pb sheet counter electrode) in 2 mol dm^{-3} H_2SO_4 solution at 20°C;

– Al_{EF} (styrene-acrylate copolymer, industrial electrophoretic coating on Al 6005-T5 alloy): 50×50×5.93 mm and

– AISI 304 SS (304/0H18N9): 30×30×5.01 mm.

All metal samples were initially degreased with ethanol, dried in exicator and weighed on a Sartorius CP224--OCE precision balance with 0.1 mg accuracy. Electrical connections to electrodes were provided by means of threaded steel wires, covered with shrinkable PE tubes (all electrode corners were properly taped with a polymer, acid resistant adhesive tape). The galvanic cells were then assembled by wire connecting the respective electrode pairs (with an electrode-to-electrode distance equal to 50 mm). The corrosion exposure was realized in 3 wt. % sodium chloride solution, prepared by dissolution of

NaCl salt (Polish Chemical Compounds, p.a.) in distilled water, in glass beakers at room temperature and an average pH value of 8 for a total period of 89 days.

Corrosion measurements for examined galvanic couplings involved intermittent recording of their mixed corrosion potentials (E_{cor}) and anode, and cathode open circuit potentials (*ocp*) measured vs. saturated calomel electrode (SCE), where sufficient time was allowed between the measurements in order for the electrodes to completely depolarize. In addition, intensity of galvanic coupling current (I_{gc}) was periodically evaluated through the so-called ZRA (zero resistance ammeter) mode of the Solartron 12.608 W Full Electrochemical System, consisting of 1260 frequency response analyzer (FRA) and 1287 electrochemical interface (EI). The latter System was also employed to carry-out occasional linear polarization experiments, which involved electrode micro-polarizations conducted at ±10 mV around the open circuit (corrosion) potential, at a scan-rate of 0.10 mV s^{-1}. On the other hand, electrode potential measurements were conducted by means of Fluke 85 III multimeter; oxygen content, electrolyte conductivity and pH evaluations were then performed with HI 9146, HI 9835 and HI 2002-01 meters from Hanna Instruments, correspondingly.

Furthermore, SEM/EDX spectroscopy analyses were carried-out for unexposed and corrosion-tested metal samples by means of Merlin FE-SEM microscope (Zeiss), equipped with Bruker XFlash 5010 EDX instrumentation (with 125 eV resolution).

RESULTS AND DISCUSSION

Spectroscopic examination of unexposed and corrosion--tested metal samples

Figures 1 through 3 and Table 1 below present the results of surface spectroscopy (SEM/EDX) examinations of fresh and the corrosion-tested (for 89 days), selected constituents of galvanic couples, namely: anodes – Magnelis®-coated (Sample A) and hot-dip Zn-coated (Sample B) steel sheets, and a cathode – oxidized Al 6063-T6 alloy (Sample C). Hence, it could be seen in Table 1 that fresh surface of Magnelis® coating is primarily composed of Zn (*ca*. 65 wt.%), Al (6%), Mg (3%), C (9%) and oxygen (14%) elements. Extended exposure of Magnelis®-coated steel electrode (Sample A) in a galvanic coupling with anodized Al 6063-T6 alloy in 3% sodium chloride solution led to a gradual depletion of zinc, aluminum and magnesium elements

Table 1. Surface EDX elemental analysis for unexposed and corrosion-tested Magnelis®-coated (Sample A), hot-dip Zn (Sample B) and oxidized Al 6063-T6 alloy (Sample C) materials

Surface Sample A (unexposed)

Element	Series	unn. C [wt.%]	norm. C [wt.%]	Atom. C [at.%]	Error (1 Sigma) [wt.%]
Carbon	K-series	8.35	9.11	24.83	1.62
Zinc	K-series	59.80	65.23	32.64	2.08
Oxygen	K-series	12.92	14.09	28.82	1.85
Aluminium	K-series	5.85	6.38	7.74	0.31
Magnesium	K-series	2.98	3.26	4.38	0.20
Silicon	K-series	0.19	0.21	0.24	0.04
Phosphorus	K-series	0.62	0.68	0.71	0.06
Chromium	K-series	0.67	0.73	0.46	0.06
Iron	K-series	0.28	0.30	0.18	0.05
Total:		91.67	100.00	100.00	

Surface Sample B (corrosion-tested)

Element	Series	unn. C [wt.%]	norm. C [wt.%]	Atom. C [at.%]	Error (1 Sigma) [wt.%]
Oxygen	K-series	32.52	35.74	60.49	3.60
Aluminium	K-series	0.08	0.09	0.09	0.03
Iron	K-series	0.11	0.12	0.06	0.03
Zinc	K-series	51.40	56.49	23.39	1.73
Carbon	K-series	6.23	6.85	15.43	0.90
Silicon	K-series	0.06	0.06	0.06	0.03
Sulfur	K-series	0.02	0.02	0.02	0.03
Chlorine	K-series	0.39	0.43	0.33	0.04
Calcium	K-series	0.18	0.19	0.13	0.03
Total:		90.99	100.00	100.00	

Surface Sample A (corrosion-tested)

Element	Series	unn. C [wt.%]	norm. C [wt.%]	Atom. C [at.%]	Error (1 Sigma) [wt.%]
Oxygen	K-series	27.75	30.06	55.37	3.11
Magnesium	K-series	2.49	2.69	3.27	0.16
Aluminium	K-series	1.73	1.88	2.05	0.11
Chlorine	K-series	0.09	0.09	0.08	0.03
Iron	K-series	1.63	1.76	0.93	0.08
Zinc	K-series	53.80	58.29	26.27	1.81
Carbon	K-series	4.31	4.67	11.45	0.68
Silicon	K-series	0.50	0.55	0.57	0.05
Sulfur	K-series	0.01	0.01	0.01	0.03
Total:		92.31	100.00	100.00	

Surface Sample C (corrosion-tested)

Element	Series	unn. C [wt.%]	norm. C [wt.%]	Atom. C [at.%]	Error (1 Sigma) [wt.%]
Oxygen	K-series	56.11	52.61	64.71	6.07
Aluminium	K-series	34.23	32.10	23.41	1.61
Zinc	K-series	9.07	8.51	2.56	0.35
Silicon	K-series	1.25	1.17	0.82	0.08
Carbon	K-series	5.37	5.04	8.25	0.83
Sulfur	K-series	0.04	0.04	0.02	0.03
Chlorine	K-series	0.13	0.12	0.07	0.03
Calcium	K-series	0.13	0.12	0.06	0.03
Iron	K-series	0.31	0.29	0.10	0.04
Total:		106.64	100.00	100.00	

Surface Sample B (unexposed)

Element	Series	unn. C [wt.%]	norm. C [wt.%]	Atom. C [at.%]	Error (1 Sigma) [wt.%]
Carbon	K-series	10.71	11.69	38.10	2.24
Zinc	K-series	72.64	79.24	47.45	2.51
Oxygen	K-series	4.87	5.32	13.01	0.99
Aluminium	K-series	0.47	0.51	0.74	0.06
Iron	K-series	0.16	0.17	0.12	0.04
Lead	M-series	2.83	3.08	0.58	0.15
Total:		91.67	100.00	100.00	

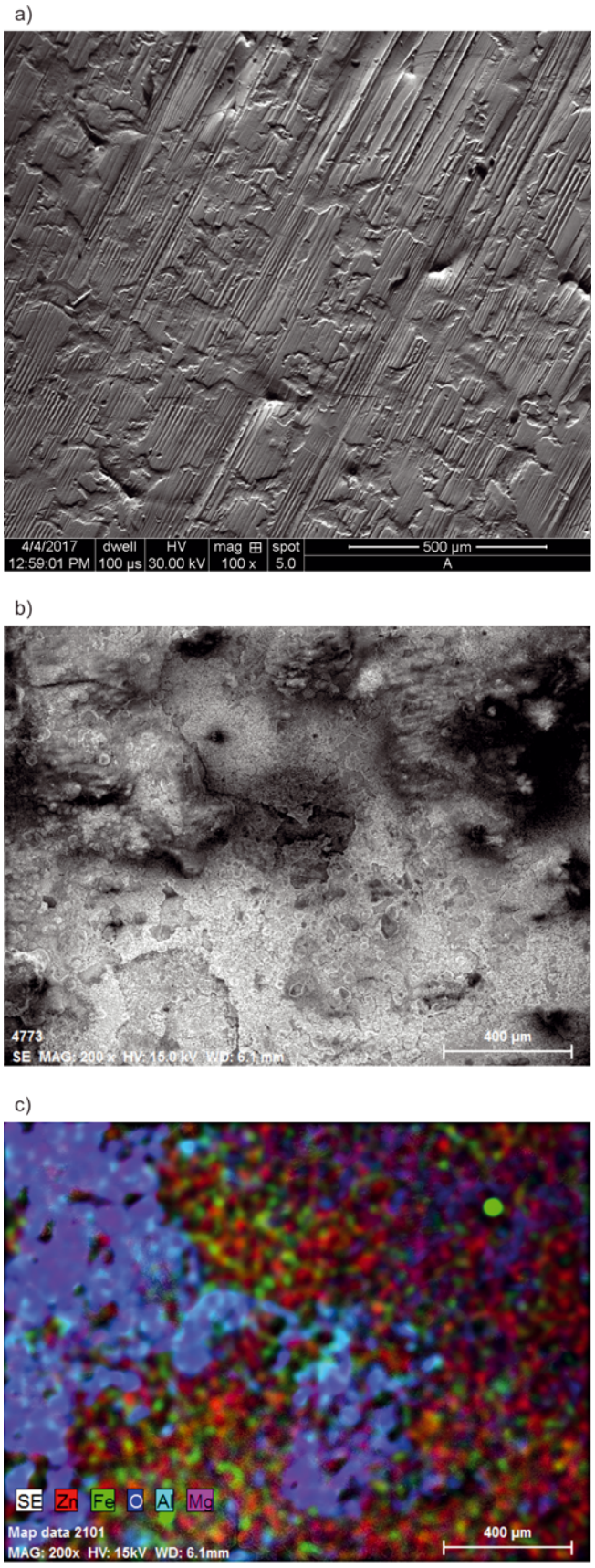

Figure 1. a) SEM micrograph picture of Magnelis®-coated carbon steel surface, taken at 100× magnification for a fresh electrode; b) As in (a) above, but taken at 200× magnification for corrosion-tested electrode; c) As in (b) above, but EDX mapping

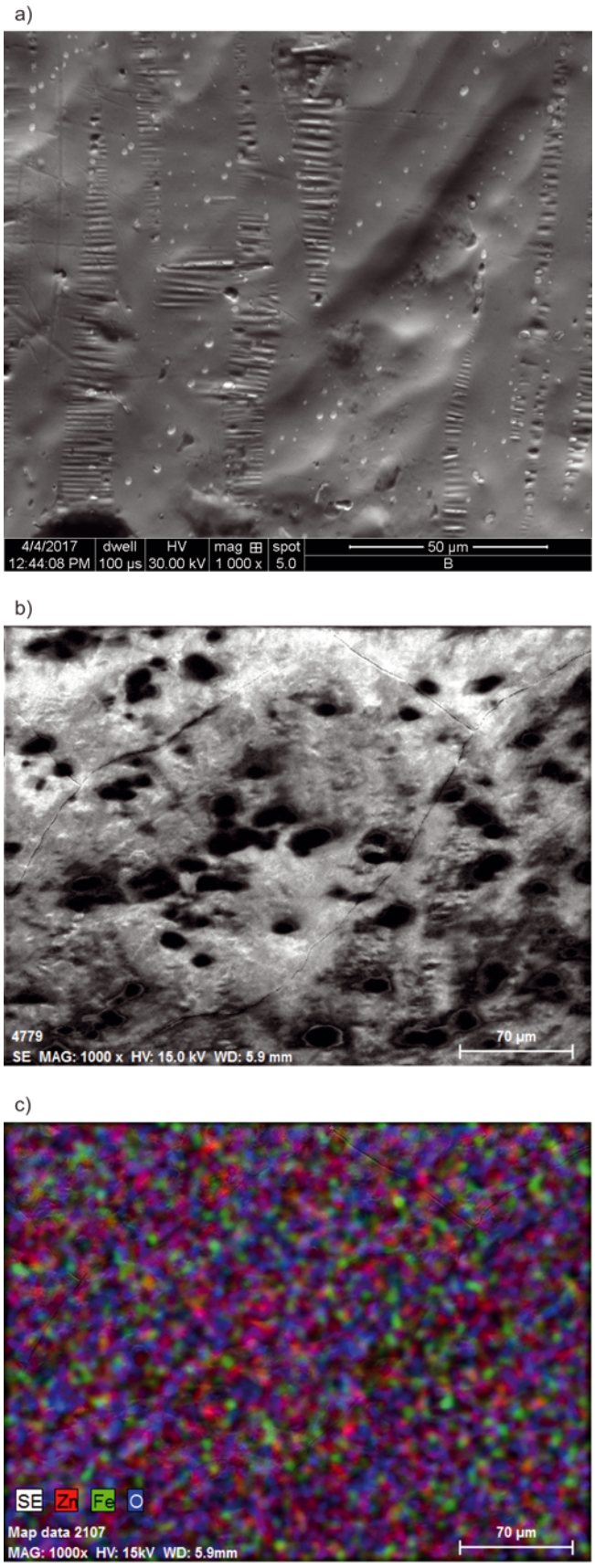

Figure 2. a) SEM micrograph picture of hot-dip Zn-coated carbon steel surface, taken at 1000× magnification for a fresh electrode; b) As in (a) above, but taken for corrosion-tested electrode; c) As in (b) above, but EDX mapping

along with a radical increase of oxygen and iron surface concentrations. The latter could be supported by the analysis of EDX elemental mapping in Figure 1c. Similar observations could be made for Sample B, where considerable surface oxidation along with the presence of Fe for NaCl-exposed electrode might clearly be discerned in the EDX micrograph picture of Figure 2c. However, the most important observation that could be deduced from

comparison of SEM micrographs of fresh Magnelis®/Zn-coated steel samples (Figs. 1a and 2a, respectively) with those of the corrosion-tested electrodes (Figs. 1b and 2b, correspondingly) is that extended electrode exposure in sodium chloride solution resulted in significant surface accumulation of porous (especially manifested in Fig. 2b) corrosion products. These deposits typically create stable surface layers, which then contribute to hampering oxygen diffusion to the metal coating. On the other hand, prolonged corrosion exposure of the cathode side (oxidized Al 6063-T6 alloy) resulted in deposition of significant amount (*ca*. 8.5 wt.%) of Zn element on the electrode surface (refer to Table 1 again and to Figs. 3a, and 3b).

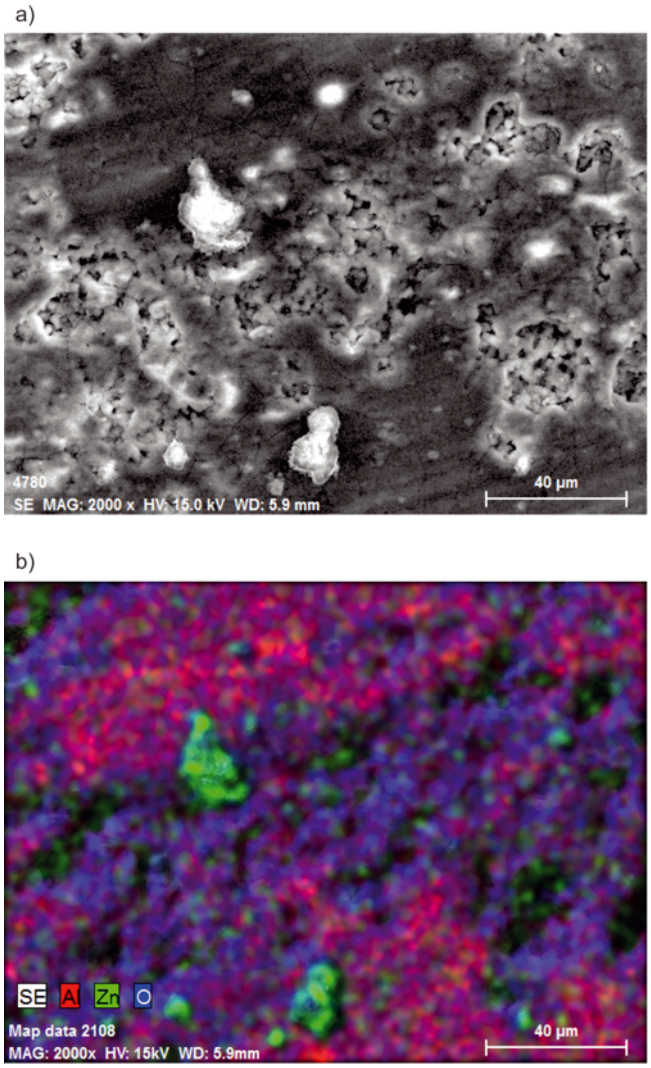

Figure 3. a) SEM micrograph picture of oxidized Al 6063-T6 alloy surface, taken at 2000× magnification for corrosion-tested electrode; b) As in (a) above, but EDX mapping

Corrosion characteristics of galvanic couplings

Initially, the corrosion performance of fresh and NaCl-exposed (after 38 days of free corrosion exposure) Magnelis® and Zn-coated carbon steel electrodes was examined by means of the linear polarization method. The latter allowed for the derivation of polarization resistance (R_p) and the corrosion current-density (j_{cor}) parameters, as shown in Table 2 below. The polarization resistance was calculated as the inverse of the slope of I (current) vs. E (potential) graph, based on above-mentioned micro-polarization measurements. The corrosion current (I_{cor}) was then derived from the well-known Stern-Geary relationship (equation 1):

$$I_{cor} = \frac{b_a b_c}{2.303 R_p (b_a + b_c)} \quad (1)$$

When Tafel slopes (b_a and b_c) of 120 mV decade^{-1} are used, this equation simplifies to $I_{cor} = 0.026 \times R_p^{-1}$. Thus, when compared to Magnelis® material, hot-dip Zn coating is characterized by significantly increased corrosion current-densities (on the order of 9 and 14 μA cm^{-2} for fresh and the corrosion-tested samples, respectively) and the reduced values of the R_p parameter – around 2860 and 1840 Ω cm^2, correspondingly (see Table 2). Obtained corrosion current-densities could then be re-calculated to linear corrosion rates (V_L), according to equation 2 below:

$$V_L = 8.76x10^6 \frac{k_{Zn} I_{cor}}{S_A d_{Zn}} \quad /\,\mu m\, year^{-1}\,/ \quad (2)$$

where: k_{Zn} is the electrochemical equivalent for Zn in /g A^{-1} h^{-1}/,
I_{cor} is measured corrosion current in /A/,
S_A is electrode's geometrical surface area in /m^2/ and
d_{Zn} is density of zinc in /kg m^{-3}/.

Hence, the linear corrosion rates assessed at an initial stage of the corrosion process in sodium chloride solution came to about 64 and 137 μm year^{-1} for Magnelis® type and hot-dip Zn coatings, correspondingly. The above implies that any of these coatings would only last about 6 months under such aggressive experimental conditions. However, it should be stressed that due to significant surface accumulation of corrosion products, comparative evaluation of corrosion rates by the loss of electrode mass (on the order of 0.2 and 0.4 wt.% for Magnelis® and hot-dip Zn coatings, respectively, in reference to Al_{ox} cathodes and the corrosion exposure period of 89 days) was not feasible.

On the other hand, the corrosion characteristics of galvanic couplings are presented in Figsures 4 and 5 below. Hence, for all galvanic couples built by connecting Magnelis® (or Zn)-coated steel sheet with aluminum electrodes, the former exhibited anodic, whereas the latter ones cathodic behaviour (see Fig. 4a). In addition, the

Table 2. Calculated average corrosion parameters for hot-dip Zn-coated and Magnelis®-coated carbon steel electrodes, in contact with 3 wt.% NaCl solution (two electrodes were examined for each composite at days: 0 and 38), obtained through linear polarization measurements (±10 mV around the *ocp*, at a sweep rate of 0.10 mV s^{-1}).

Materials	E_{cor}/mV	R_p/Ω cm^2	j_{cor}/µA cm^{-2}
Magnelis® (d = 0)	–1052	6083	4.3
Magnelis® (d = 38)	–1058	3423	7.6
Hot-dip Zn (d = 0)	–1054	2857	9.1
Hot-dip Zn (d = 38)	–1036	1836	14.2

corrosion potential (E_{cor}= –1025 to –1036 mV) approached open circuit potential of respective anodes, giving evidence that oxygen reduction reaction (equation 3) on the surface of aluminum cathode constitutes the corrosion control step[9–12].

$$O_2 + 2H_2O + 4e^- \rightarrow 4\,OH^- \quad (3)$$

Furthermore, major corrosion product for zinc coating involves formation of zinc hydroxide (stabilized by increased pH value upon the cathodic reaction), which then becomes converted to ZnO, according to equation 4:[9, 10, 13–15]

$$Zn^{2+} + 2\,OH^- \rightarrow Zn(OH)_{2(s)} \rightarrow ZnO_{(s)} + H_2O \quad (4)$$

The presence of Mg and Al additives within Magnelis® coating also leads to the formation of other and complex corrosion products (see e.g. Refs. 10 and 13 for details). The lowest value of the galvanic current-density parameter (*ca*. 0.04 μA cm^{-2} upon 89 days of the exposure, see Fig. 4b) was exhibited by the Cell 1 (Magnelis®-coating as anode vs. oxidized Al cathode), which also coincided with the minimum *ocp* potential difference between the electrodes (about 27 mV, Fig. 4a). Progressive cathodic polarization of the aluminum cathodes observed for both Magnelis®-based galvanic

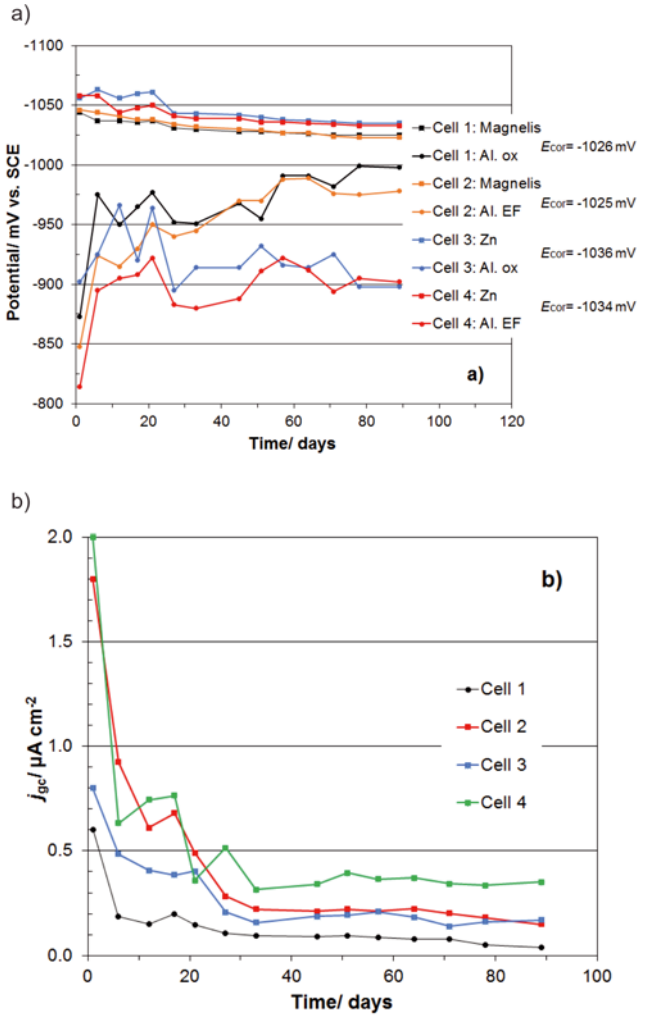

Figure 4. a) Open circuit and corrosion potentials in function of exposure time for corrosion-tested galvanic couplings (Cells 1 through 4) in 3 wt.% NaCl solution; b) As in (a) above, but galvanic couple current-density for stated Cells in function of exposure time

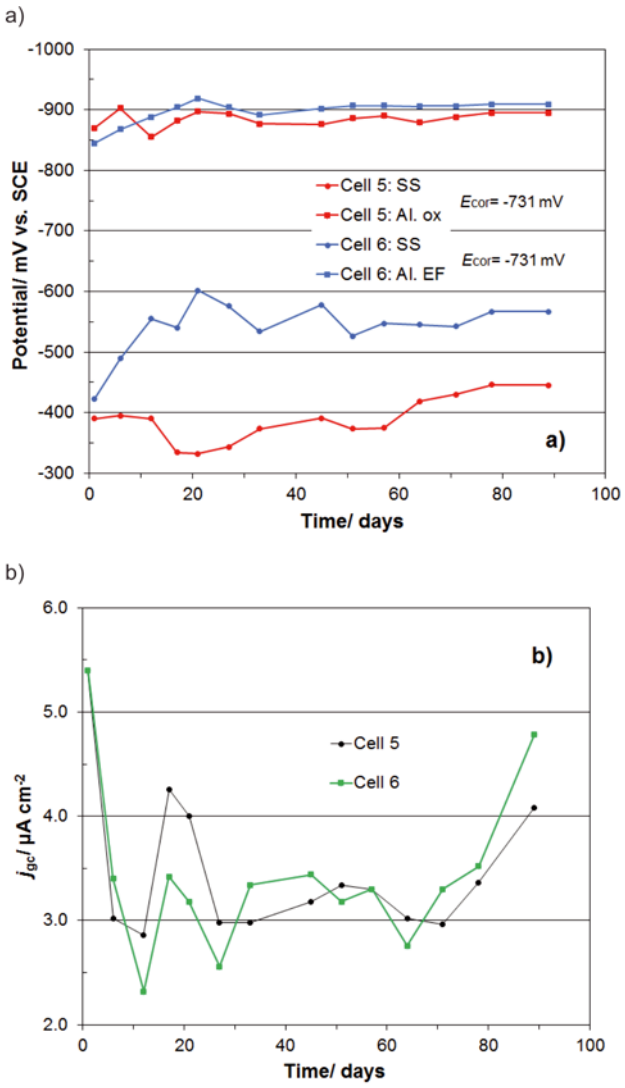

Figure 5. a) Open circuit and corrosion potentials in function of exposure time for corrosion-tested galvanic couplings (Cell 5 and Cell 6) in 3 wt.% NaCl solution; b) As in (a) above, but galvanic couple current-density for stated Cells in function of exposure time

cells most likely results from increased deposition of Zn (or perhaps also Mg) element on the Al surface, as previously shown in Figures 3a and 3b and Table 1.

In order to assess the effect of galvanic coupling current on the rate of general corrosion for Magnelis®-type and hot-dip Zn coatings, average values of the I_{gc} parameter for the Cells 1 through 4 become incorporated into the equation 2 to derive the corresponding linear corrosion rates for these coatings. Thus, the calculated corrosion rates came to: 1.6, 3.2, 2.7 and 5.5 μm year^{-1} for the Cells: 1, 2, 3 and 4, respectively. In other words, under experimental conditions (3% NaCl, pH range: 7.9–8.3, temperature: 16–18°C, dissolved [O_2] = 7.1–7.3 ppm and electrolyte conductivity, $\varkappa$ = 30–35 mS cm^{-1}), the increase of general corrosion rate due to galvanic coupling is insignificant and comes to about 3.7% for Magnelis® and 3.0% for the hot-dip Zn coating.

On the contrary, the Cells denoted as 5 and 6 (SS cathode vs. Al_{ox}/Al_{EF} anode) exhibited radically larger *ocp* voltages (Fig. 5a) and galvanic current-densities (Fig. 5b) than those recorded for the Cells 1 through 4. As a result, the calculated linear corrosion rate (due to the galvanic coupling effect) for aluminum anode

(with appropriate changes of k and d parameters in equation 2 in order to account for Al) approached 40 μm year^{-1}, where $Al(OH)_3$ is a major corrosion product[11] (equation 5):

$$4Al + 3O_2 + 6H_2O \rightarrow 4Al(OH)_3 \quad (5)$$

In addition, the corrosion process in the case of SS/Al galvanic cells is also controlled by the cathodic reduction of oxygen (compare the recorded mixed corrosion potential value of –731 mV with those of the corresponding open circuit anode potentials in Fig. 5a).

CONCLUSIONS

Zinc-coated steel and aluminum sheets, and stainless steel fasteners are regularly used structural materials to build ground-mounted photovoltaic power stations. Laboratory-based galvanic coupling experiments conducted in 3 wt.% NaCl, self-aerated solution confirmed that the galvanic coupling currents produced by Zn(Magnelis®)-coated steel coupled with aluminium cathodes stand just for several per-cent of the corrosion rate increase. In addition, Magnelis® coating exhibits significantly reduced corrosion rates, as compared to regular hot-dip zinc coating. The latter proves to be in effect for both examined galvanic couples, as well as freely corroding Zn-based metal coatings, which is most likely the effect of surface formation of more insoluble and less permeable to oxygen corrosion products, favoured by Magnelis®'s Mg and Al additives.

Hence, from the technical point of view it seems rather safe to use electrically connected Zn (or Magnelis®) coatings with Al surfaces under employed experimental conditions. However, it should also be understood that variable environmental conditions (e.g. sporadic removal of surface corrosion deposits by rainfall, changing pH and dissolved oxygen level for atmospheric precipitation) could periodically (and significantly) increase the galvanic coupling currents.

On the other hand, galvanic couples between stainless steel and aluminum parts should rather be avoided in practice. These cells revealed radically greater current--densities, where sole galvanic coupling effect for aluminum loss could be estimated at 40 μm year^{-1}.

LITERATURE CITED

1. Aste, N. & Pero, C.D. (2010). Technical and economic performance analysis of large-scale ground-mounted PV plants in Italian context. *Prog. Photovoltaics* 18(5), 371–384. DOI: 10.1002/pip.984.

2. Desideri, U., Proietti, S., Zepparelli, F., Sdringda, P. & Bini, S. (2012). Life cycle assessment of a ground-mounted 1778 kW_p photovoltaic plant and comparison with traditional energy production systems. *Appl. Energy* 97, 930–943. DOI: 10.1016/j.apenergy.2012.01.055.

3. Yang, R.J. (2015). Overcoming technical barriers and risks in the application of building integrated photovoltaics (BIPV): hardware and software strategies. *Automat. Constr*. 51, 92–102. DOI: 10.1016/j.autcon.2014.12.005.

4. Fontana, M.G. (1987). Corrosion Engineering, 3rd ed., McGraw-Hill, New York, Chapter 3, p. 39.

5. Roberge, P.R. (2000). Handbook of Corrosion Engineering, McGraw-Hill, New York, Chapter 5, p. 340.

6. Uhlig, H.H. & Revie, R.W. (1985). Corrosion and Corrosion Control: An Introduction to Corrosion Science and Engineering, 3rd ed., John Wiley & Sons, New York, Chapter 6, p. 101.

7. Kautek, W. (1988). The galvanic corrosion of steel coatings: aluminum in comparison to cadmium and zinc. *Corr. Sci*. 28(2), 173–199. DOI: 10.1016/0010-938X(88)90094-7.

8. *Magnelis®*, industry.arcelormittal.com/magnelis, last accessed (07/04/2017).

9. Hamlaoui, Y., Pedraza, F. & Tifouti, L. (2007). Comparative study by electrochemical impedance spectroscopy (EIS) on the corrosion resistance of industrial and laboratory zinc coatings. *Am. J. Appl. Sci*. 4(7), 430–438. DOI: 10.3844/ajassp.2007.430.438.

10. Salgueiro Azevedo, M., Allely, C., Ogle, K. & Volovitch, P. (2015). Corrosion mechanisms of Zn(Mg, Al) coated steel in accelerated tests and natural exposure: 1. The role of electrolyte composition in the nature of corrosion products and relative corrosion rate. *Corr. Sci*. 90, 472–481. DOI: 10.1016/j.corsci.2014.05.014.

11. Hakansson, E., Hoffman, J., Predecki, P. & Kumosa, M. (2017). The role of corrosion product deposition in galvanic corrosion of aluminum/carbon systems. *Corr. Sci*. 114, 10–16. DOI: 10.1016/j.corsci.2016.10.011.

12. Sun, H., Liu, S. & Sun, L. (2013). A comparative study on the corrosion of galvanized steel under simulated rust layer solution with and without 3.5 wt.% NaCl. *Int. J. Electrochem. Sci*. 8, 3494–3509.

13. Diler, E., Rouvellou, B., Rioual, S., Lescop, B., Nguyen Vien, G. & Thierry, D. (2014). Characterization of corrosion products of Zn and Zn–Mg–Al coated steel in a marine atmosphere. *Corr. Sci*. 87, 111–117. DOI: 10.1016/j.corsci.2014.06.017.

14. Hamlaoui, Y., Pedraza, F. & Tifouti, L. (2008). Corrosion monitoring of galvanised coatings through electrochemical impedance spectroscopy. *Corr. Sci*. 50, 1558–1566. DOI: 10.1016/j.corsci.2008.02.010.

15. Liu, Y., Li, H. & Li, Z. (2013). EIS Investigation and Structural Characterization of Different Hot-Dipped Zinc-Based Coatings in 3.5% NaCl Solution. *Int. J. Electrochem. Sci*. 8, 7753–7767.